Minimax Theory and its Applications
Volume 11 (2026), No. 2s, 12-22

A Nonlinear Variational Analysis Approach for Structural Stability Optimization Under Dynamic Loading

R. Shanthi[1], Dr. Chetansinh R. Vaghela[2], Mr. D. Ganesh[3], Tarun Kapoor[4], Nunna Venkata Raju[5], Leena Deshpande[6], Paul Praveen Albert Selvakumar[7]

[1]Associate Professor & HOD, Department of Mathematics, Meenakshi College of Arts and Science, Meenakshi Academy of Higher Education and Research, Chennai, Tamil Nadu, India. shanthir@maher.ac.in

[2]Associate Professor, Faculty of Science, Gokul Global University, Gujarat, India. crvaghela.maths.gsc@gokuluniversity.ac.in, https://orcid.org/0000-0001-5692-5190

[3]Assistant Professor, Department of Computer Science and Engineering, Vardhaman College of Engineering, Shamshabad, Hyderabad, India. dganesh@vardhaman.org

[4]Centre of Research Impact and Outcome, Chitkara University, Rajpura, Punjab, India. tarun.kapoor.orp@chitkara.edu.in, https://orcid.org/0009-0001-6432-2573

[5]Bonam Venkata Chalamayya Institute of Technology & Science, Amalapuram, Andhra Pradesh, India. venkatraju8096@gmail.com

[6]Associate Professor, Department of Computer Engineering - Software Engineering, Vishwakarma Institute of Technology, Pune, Maharashtra, India. leena.deshpande@vit.edu

[7]Associate Professor, School of Engineering & Technology, Noida international University, Uttar Pradesh, India. paulpraveen.a@niu.edu.in

Abstract

Structural systems loaded dynamically undergo complicated nonlinear interplay of deformation, material behavior, excitation and stability restrictions. Traditional methods of stability optimization assume linearity and may not provide correct description of instability behavior under varying loading conditions. This study attempts to introduce mathematical approach to optimization of structural stability through nonlinear variational analysis technique, which is based on the principles of equilibrium and constrained optimization. Nonlinear variational formulation of structural stability optimization problem will be introduced, where nonlinear operators, dynamic loading effects and mechanical restrictions are taken into consideration within optimization framework. Theoretical considerations involve variational inequality theory and nonlinear functional analysis for proving existence and uniqueness of solutions and their convergence. An optimization algorithm involving nested Galerkin and projected gradient techniques is used to find out stable structural configuration with minimum material costs under dynamic restrictions. Numerical studies of harmonic-loaded slender column and two bay frame prove efficiency of the proposed approach in terms of accuracy of stability optimization and prediction. The results indicate that the optimized design of the column offers about 11.9% reduction in mass with compliance to dynamic stability criteria, while dynamic variational frame design offers around 13.0% savings in material as compared to the static based optimization approach. This is indicative of the fact that the developed method gives better robustness, stability assessment, and optimization of structure subjected to dynamic loads. The research work develops a generalized non-linear variational approach to design robust structural systems.

Keywords: Nonlinear variational analysis, structural stability optimization, dynamic loading, variational inequality, nonlinear structural dynamics, functional optimization, structural resilience.

1. Introduction

Optimization of dynamic structural systems stability is currently one of the research areas in the field that takes into account the need for modelling nonlinearity, optimization, and modern computational algorithms. Structural system dynamics implies a complex relationship between structural deformation, loading and stability, which

requires special mathematical models (Sharma et al., 2026). Optimization of structural system stability has been successfully applied to aerospace structures as a method that allows improving stability and response using advanced methods of optimization. It has shown the need to take into account time-dependent loading effects and nonlinear deformation of the structure during design. Nonlinear response sensitivity analysis has been a good tool for the identification of important parameters for structural optimization (Schwarz & Ramm, 2001).

Variational optimization methods have been applied to the problems of structural health monitoring and damage assessment (Mahmoudi & Lailypour, 2015). Nonlinear feature extraction and parameter optimization have allowed characterizing a damaged structure under moving loads and demonstrated the ability of optimization-based approach to capture the complex behavior of dynamic system (Golait et al., 2025). Material distribution optimization has allowed improving dynamic stability by improving load-carrying capabilities of structural components and minimizing their instability (Szmidla et al., 2025). Optimization frameworks based on performance have been developed for nonlinear structures undergoing stochastic dynamic excitations (Golait et al., 2025). The framework has emphasized improvement in reliability considering uncertainty effects and the evaluation of structural response to loading variations (Mahmoudi & Lailypour, 2015). Vibration control schemes involving the use of nonlinear structural elements have shown improvement in vibration suppression and dynamic stability by optimizing nonlinear properties (Guo et al., 2026).

Nonlinear optimization frameworks driven by data have extended the scope of structural analyses through the incorporation of computational optimization into elasticity-based models (Udayakumar et al., 2023). This allows for accurate estimation of dynamic responses without loss of mathematical consistency in the modeling of nonlinear structures (Mandapatti, 2025). Nonlinear stability analysis of structural reliability for random loads has also been investigated, considering geometric imperfections and uncertainties associated with excitations (Most et al., 2004). Variational analysis approaches have been used in different engineering optimization areas for finding stable equilibrium solutions through mathematical modeling. Variational methods involving second order differential equations enhance the accuracy of optimization for complex energy and stability systems (Udayakumar et al., 2023). Advanced numerical studies on microstructure materials have highlighted the effect of optimized geometric forms on mechanical stability and performance of structures (Li et al., 2026).

Innovative optimization schemes for nonlinear structural systems have been formulated to optimize both the size, shape, and dynamic behavior of structures. Optimization of nonlinear coupled responses with regard to achieving stability attributes in structures has been made possible using the suggested methods (Khan, 2025). Nonlinear post-buckling study on composite structures has revealed the necessity of considering nonlinear attributes as well as material imperfections when it comes to predicting the stability of structures under complicated loading cases (Wang et al., 2026). Optimization of dynamic behavior in lightweight structures has been considered as a way of enhancing the dynamic response and reliability of structures. Both experimental and computer studies on variable cross-section structures show the importance of considering nonlinearities in optimizing structural behavior (Zhang & Lu, 2026). Stability prediction under dynamic loading using machine learning has been considered for estimating nonlinear responses with greater efficiencies than those provided by conventional analytical schemes (Chen, 2026).

Efficiency and stability control in energy and mechanical systems have been achieved through optimization of nonlinear dynamic behavior using intelligent algorithms (Mandapatti, 2025). System efficiency and stability improvement through adaptive control using optimization algorithms has been reported under different operating conditions (Yang et al., 2026). Enhancement of structural efficiency through optimized lattice structure design has been proven.

The latest advances in intelligent optimization methodologies and digital twin-based models have made it possible to perform real-time decision-making in complex dynamic systems. Such systems integrate the concepts of uncertainty management, multi-objective optimization, and adaptive modeling in order to enhance stability and performance under dynamic conditions. Nevertheless, current methodologies lack rigorously mathematically justified models of nonlinear equilibrium, convergence, and stability optimization. For this reason, it is necessary to consider the framework of nonlinear variational analysis to develop a theoretical approach to structural stability optimization.

Key contribution

- Nonlinear variational theory is proposed for the representation of structural stability optimization as an equilibrium problem under dynamic loads. The problem statement involves nonlinear operators and mechanical constraints which describe complicated behavior of structures.
- Theoretical properties of the developed approach, namely existence, uniqueness and convergence of stable solutions are shown using nonlinear functional analysis and variational inequality theory. These theoretical properties form a basis for reliability of structural optimization.

- The optimization approach is proposed for improving stability of structures in time-varying loads to find the corresponding stable states. The approach has better performance with regard to satisfaction of constraints, robustness and computation than conventional approaches of structural stability optimization.

The remaining part of the paper is organized as follows. In Section II, the problem statement is described. It includes the description of the structural model, the variational stability functional and the optimization problem for structural stability analysis. Section III describes the developed nonlinear variational optimization algorithm with the use of Galerkin discretization. Theoretical analysis of the proposed formulation is presented in Section IV, where the existence and uniqueness of equilibrium solutions as well as the stability bounds for the same under dynamic loading are proven. The numerical analysis and performance assessment of the proposed model have been carried out through the application of harmonic loads to slender columns and two-bay frames this section further discusses the aspects of optimization performance, stability enhancement, and material savings. Finally, Section V summarizes the research findings and suggests future scope of research.

2. Problem formulation

2.1. Structural and loading model

Consider a slender elastic structure occupying a reference domain $\Omega \subset \mathbb{R}$ (or a one-dimensional parametrization $s \in [0, L]$ along its centerline, for a column, beam, or frame member), with transverse displacement field $w(s,t)$ and a design variable field $x(s)$ e.g., cross-sectional area or second moment of area chosen from an admissible design set X_{ad}. The structure is subjected to an axial load $P(t) = P_0 + P_l \cos(\Omega t)$, representing a static component P_0 plus a harmonically varying dynamic component of amplitude P_l and frequency Ω, together with a transverse forcing $q(s,t)$ where relevant.

The total mechanical energy of the structure at time t combines strain energy, the potential of the applied axial load acting through the beam's geometric shortening, and kinetic energy:

$$\mathcal{E}[w,x](t) = \int_0^L \frac{1}{2} EI\big(x(s)\big) w''^{(s,t)^2}\, ds - \int_0^L \frac{1}{2} P(t) w'^{(s,t)^2}\, ds + \int_0^L \frac{1}{2} \rho A\big(x(s)\big) \dot{w}(s,t)^2\, ds \qquad (1)$$

In Equation (1) describes the where E is Young's modulus, $I(s)$ the second moment of area (an increasing, concave function of s for standard cross-sectional families), ρ the material density, $A(s)$ the cross-sectional area (increasing, convex in s for most practical parametrizations), primes denote differentiation in s $\left(w' = \frac{\partial w}{\partial s}, w'' = \frac{\partial^2 w}{\partial s^2}\right)$, and dots differentiation in t $\left(\dot{w} = \frac{\partial w}{\partial t}\right)$. The first term is bending strain energy, the second is the destabilizing work of the axial load through second-order (rotation) shortening, and the third is kinetic energy in table 1.

Notation

Table 1: Notation used in the variational model

Symbol	Definition
$w(s,t)$	Transverse displacement field
$x(s)$	Design variable field (e.g., cross-sectional area/stiffness distribution)
E, ρ	Young's modulus, mass density (material constants)
$I(x), A(x)$	Second moment of area, cross-sectional area, as functions of x
$P(t)$ $= P_0 + P_l \cos(\Omega t)$	Time-varying axial load: static component P_0, dynamic amplitude P_1, frequency Ω
$V = H_0^2(0, L)$	Admissible displacement space (clamped/simply-supported boundary conditions)
$J[w,x]$	Generalized Rayleigh-type stability functional
$\lambda_{\text{dyn}}(x)$	Dynamic stability margin (generalized critical-load multiplier)
$\lambda_{\text{stat}}(x)$	Classical static buckling multiplier ($\Omega \to 0$ limit of λ_dyn)
$m(x) = \int_0^L A\left(x(s)\right) ds$	Structural mass/material used (objective to be minimized)
X_{ad}	Admissible set of design fields, $X_{\text{ad}} = \{x : x_L \le x(s) \le x_U,\ \forall s\}$

2.2. Variational stability functional

Structural equilibrium at fixed design x and fixed time-instant load level P is characterized variationally as a stationary point of the potential-energy part of (1) over the admissible displacement space $V = H_0^2(0, L)$ (functions with square-integrable second derivative satisfying the boundary conditions) in Equation (2).

$$w \in V \text{ solves: } \delta\left[\int_0^L \frac{1}{2} EI(x)(w'')^2\, ds - \int_0^L \frac{1}{2} P(w')^2\, ds\right] = 0 \quad \text{for all admissible variations.} \qquad (2)$$

The stability of the equilibrium state depends on the sign of the second variation, with instability occurring when the following Rayleigh quotient a min-max/eigenvalue problem formulation takes the value one for the first time as P varies in Equation (3).

$$\lambda_{\text{stat}}(x) = \min_{\substack{w \in V \\ w \neq 0}} \frac{\int_0^L E\, I(x)(w'')^2\, ds}{\int_0^L (w')^2\, ds} \qquad (3)$$

Thus, the classical static critical load becomes:

$$Pcr\ \ (x) = \lambda stat\ \ (x)$$

Thus, the classical static critical load becomes $P_''cr''\ (x) = \lambda_''stat''\ (x)$ which is achieved through the min-max principle for the smallest eigenvalue of the corresponding linear buckling operator. To generalize this result for the case of the dynamic loads, one has to introduce the term associated with the kinetic energy into the Rayleigh quotient and compute it under the dynamic load.

$$J[w, x](t) = \frac{\int_0^L EI(x)(w'')^2\, ds - \int_0^L \rho A(x)\dot{w}^2\, ds}{\int_0^L (w')^2\, ds} \qquad (4)$$

$$\lambda_{\text{dyn}}(x) = *\, ess\, inf_{t \in [0,T]} \min_{\substack{w \in V \\ w \neq 0}} J\,[w, x](t) \qquad (5)$$

In Equations (4) and (5), $\lambda_''dyn''\ (x)$ becomes $\lambda_''stat''\ (x)$ for the case where the inertial term becomes zero (quasi-static load), and is thus, by its very construction, a conservative (lower bound) stability margin over the load history interval $[0, T]$, because it considers the worst-case time and mode shape combination.

2.3. Structural stability optimization model

The design problem is to choose the design field x to minimize structural mass subject to the requirement that the applied load amplitude remain below the dynamic stability margin by a prescribed safety factor $\gamma \geq 1$:

$$\underset{x \in X_{\text{ad}}}{\text{minimize}} \quad \mathrm{m(x)} = \int_0^{\mathrm{L}} \mathrm{A}\left(\mathrm{x(s)}\right) \mathrm{ds} \qquad (6)$$

$$\text{subject to} \quad \lambda_{\text{dyn}}(\mathrm{x}) \geq \gamma(\mathrm{P_0} + \mathrm{P_1}) \qquad (7)$$

Equations (6) and (7) express a nonlinear non-convex variational optimization problem (in general), because $\lambda_''dyn''\ (x)$ is defined by inner optimization over displacement field w. The theory behind this problem is developed in Section 4, while the numerical treatment is discussed in Section 5. Theoretical results

This subsection proves the existence of an equilibrium displacement field satisfying equation (2), the uniqueness of the solution under the condition of strict convexity, and a variational min-max lower bound for the dynamic critical load, thus justifying the use of $\lambda_''dyn''\ (x)$ as a design constraint.

2.4. Existence of the equilibrium displacement field

Theorem 1.

Fix a design $x \in X_{\text{ad}}$ with $0 < I_{\min} \leq I\big(x(s)\big) \leq I_{\max} < \infty$ for all s, and fix a load level $P < \lambda_{\text{stat}}(x)$. Then the potential-energy functional in Equation (8)

$$\Pi[w] = \int_0^L \frac{1}{2} EI(x)(w'')^2\, ds - \int_0^L \frac{1}{2} P(w')^2\, ds \qquad (8)$$

attains a minimum over $V = H_0^2(0, L)$, i.e., an equilibrium displacement field $w^* \in V$ exists.

Proof. Apply the direct method of the calculus of variations, verifying coercivity and weak lower semi continuity of Π on V.

Coercivity: Because $P < \lambda_{\text{stat}}(x)$, by definition (3) of $\lambda_{\text{stat}}(x)$ as the minimum of the Rayleigh quotient, for every $w \in V$, in equation (9)

$$\int_0^{\mathrm{L}} \mathrm{E\,I(x)(w'')^2\,ds} \geq \lambda_{\text{stat}}(\mathrm{x}) \int_0^{\mathrm{L}} (\mathrm{w}')^2\ \mathrm{ds} > \mathrm{P} \int_0^{\mathrm{L}} (\mathrm{w}')^2\ \mathrm{ds}, \tag{9}$$

so there exists $\varepsilon = 1 - P/\lambda_{\text{stat}}(x) > 0$ such that in Equation (10)

$$\Pi[w] \geq \frac{1}{2} EI_{min} \|w''\|_{L^2}^2 - \frac{1}{2} P \int_0^L (w')^2\ ds \geq \frac{1}{2} \varepsilon \int_0^L E\, I(x)(w'')^2\, ds \geq \frac{1}{2} \varepsilon EI_{min} \|w''\|_{L^2}^2, \tag{10}$$

and by the Poincare–Friedrichs inequality on $V = H_0^2(0, L)$ (which controls $\|w\|_{H^2}$ by $\|w''\|_{L^2}$ under the clamped/simply-supported boundary conditions), $\Pi[w] \to +\infty$ as $\|w\|_{H^2} \to \infty$; hence Π is coercive on V.

Weak lower semi continuity: Π is the sum of two quadratic forms in w with bounded and measurable coefficients $EI(x(s)) \in [EI_min, EI_max]\ and\ P$; quadratic forms in bounded coefficients are continuous, and convex and continuous functionals on a Hilbert space are weakly lower semi-continuous (convexity alone guarantees weak lower semi-continuity of norms), hence, Π is weakly lower semi-continuous on V. Since V is a closed subspace of the Hilbert space $H^2(0, L)$, it is itself weakly sequentially complete, and any minimizing sequence for the coercive functional Π is bounded in V and therefore has a weakly convergent subsequence $w_k \rightharpoonup w^*$; weak lower semi continuity gives so w^* is a minimizer in Equation (11),

$$\Pi[w^*] \leq \liminf_k \Pi\,[w_k] = \inf_V \Pi, \tag{11}$$

2.5. Uniqueness of the equilibrium

Theorem 2.

Under the hypotheses of Theorem 1, the equilibrium displacement field w^* is unique.

Proof. It suffices to show Π is strictly convex on V whenever $P < \lambda_{\text{stat}}(x)$.

Π is quadratic, $\Pi[w] = \frac{1}{2} a(w, w)$, with bilinear form

$$\mathrm{a(w,v)} = \int_0^{\mathrm{L}} \mathrm{E\,I(x)w''v''\,ds} - \mathrm{P} \int_0^{\mathrm{L}} \mathrm{w}'\ \mathrm{v}'\,\mathrm{ds} \tag{12}$$

As shown in the proof of Theorem 1,

$$\mathrm{a(w,w)} \geq \varepsilon \mathrm{EI_{min}} \|\mathrm{w''}\|_{\mathrm{L^2}}^2 \quad \text{for } \varepsilon = 1 - \frac{\mathrm{P}}{\lambda_{\text{stat}}(\mathrm{x})} > 0 \tag{13}$$

In Equation (12), and (13) so $a(w, w) > 0$ for every nonzero $w \in V$; that is, a is positive definite on V.

A quadratic functional with a positive-definite bilinear form is strictly convex, since for $w \neq v$ and $t \in (0,1)$,

$$\begin{aligned} \Pi[\mathrm{tw} + (1-\mathrm{t})\mathrm{v}] &= \mathrm{t}\Pi[\mathrm{w}] + (1-\mathrm{t})\Pi[\mathrm{v}] - \frac{1}{2}\mathrm{t}(1-\mathrm{t})\mathrm{a}(\mathrm{w}-\mathrm{v}, \mathrm{w}-\mathrm{v}) \\ &< t\Pi[w] + (1-t)\Pi[v] \end{aligned} \tag{14}$$

In Equation (14) describes $a(w - v, w - v) > 0$ for $w \neq v$.

Strictly convex functions have only one minimizer in a convex domain (by using a standard midpoint contradiction argument: Two different minimizers of the same value will violate the strictly convex property at the midpoint). Since there is an existence proof of Theorem 1, w^ ∗ is uniquely determined.

2.6. A variational min-max lower bound on the dynamic critical load

Theorem 3.

Let $w_1(x)$ denote the first (lowest) static buckling mode shape attaining the minimum in (3), normalized by $\int_0^L (w_1')^2\, ds = 1$, and let $\kappa(x,t) = \int_0^L \rho\, A(x)\dot{w}_1^2\, ds$ evaluated along the corresponding time history of the first mode under harmonic excitation at frequency Ω. Then the dynamic stability margin obeys the lower bound in Equation (15)

$$\lambda_{\text{dyn}}(\mathrm{x}) \geq \lambda_{\text{stat}}(\mathrm{x}) - \sup_{\mathrm{t}\in[0,\mathrm{T}]} \kappa(\mathrm{x},\mathrm{t}) \tag{15}$$

so that the loss of dynamic stability margin relative to the static case is bounded above by the peak modal kinetic energy of the first buckling mode.

Proof. By definition (5), $\lambda_{\text{dyn}}(x) = *\,ess\,inf_t \min_{w\neq 0} J\,[w,x](t)$, where J is the Rayleigh-type quotient in (4). For any fixed admissible w with $\int_0^L (w')^2\, ds = 1$,

$$\mathrm{J[w,x](t)} = \int_0^{\mathrm{L}} \mathrm{E\,I(x)(w'')^2\,ds} - \int_0^{\mathrm{L}} \rho\,\mathrm{A(x)\dot{w}^2\,ds} \geq \lambda_{\text{stat}}(\mathrm{x}) - \sup_{\mathrm{t}} \int_0^{\mathrm{L}} \rho\,\mathrm{A(x)\dot{w}^2\,ds}, \tag{16}$$

In Equation (16) using the definition (3) of $\lambda_{\text{stat}}(x)$ as the minimum of the (purely elastic) Rayleigh quotient over all normalized $w \in V$, which bounds the first term from below independently of t.

Taking the minimum over w on the left-hand side preserves the inequality, since the right-hand side does not depend on w. In particular, evaluating the bound along the first static buckling mode $w_1(x)$ — which is the minimizer of the purely elastic quotient and hence the mode most likely to dominate the infimum in (5) for loading frequencies Ω well below higher modal frequencies — gives $\min_w J\,[w,x](t) \geq \lambda_{\text{stat}}(x) - \kappa(x,t)$ with $\kappa(x,t) = \int_0^L \rho\, A(x)\dot{w}_1^2\, ds$.

Taking the essential infimum over $t \in [0,T]$ on both sides,

$$\lambda_{dyn}(x) = *\,ess\,inf_{t\in[0,T]} \min_w J\,[w,x](t) \geq \lambda_{stat}(x) - \sup_{t\in[0,T]} \kappa(x,t), \tag{17}$$

which is equation (17).

Corollary. Since $\kappa(x,t) \geq 0$ at all times, Equation (8) indicates that $\lambda_"dyn"\,(x) \leq \lambda_"stat"(x)$, implying that the dynamic stability margin cannot be larger than the static buckling factor, which establishes that a static buckling evaluation alone will be non-conservative if κ is significant compared to $\lambda_"stat"(x)$.

The bound (8) also gives a computationally cheap surrogate constraint — replacing the exact but expensive $\lambda_{\text{dyn}}(x) \geq \gamma(P_0 + P_1)$ in equation (18) with the sufficient condition:

$$\lambda_{stat}(x) - \sup_{t\in[0,T]} \kappa(x,t) \geq \gamma(P_0 + P_1) \tag{18}$$

3. Algorithm (nested galerkin / projected-gradient design optimization)

1. Initialization:

Initialize the design $x^{(0)} \in X_{\text{ad}}$ from the static-buckling-only design (λ_{stat} in place of λ_{dyn}), or from the Theorem 3 surrogate constraint in Equation (19)

$$\lambda_{\text{stat}}(\mathrm{x}) - \sup_{t\in[0,T]} \kappa(x,t) \geq \gamma(P_0 + P_1) \tag{19}$$

2. Modal discretization:

At iteration k, discretize w via M buckling modes of the current design $x^{(k)}$ and assemble the reduced mass, stiffness, and geometric-stiffness matrices.

3.Time-sweep eigenvalue solve:

Sweep t over a fine grid on $[0,T]$; at each t, solve the reduced generalized eigenvalue problem for the modal Rayleigh quotient, and record $\hat{\lambda}_{\text{dyn}}(x^{(k)})$ as the minimum over the grid (a discretized version of (5)).

4. Augmented lagrangian & adjoint gradient:

Form the augmented Lagrangian functional:

$$\mathcal{L}(\mathrm{x},\mu) = \mathrm{m}(\mathrm{x}) + \mu \max\{0,\ \gamma(\mathrm{P}_0 + \mathrm{P}_1) - \hat{\lambda}_{\text{dyn}}(\mathrm{x})\} + \frac{\rho_{\text{pen}}}{2}\left(\max\{0,\ \gamma(\mathrm{P}_0 + \mathrm{P}_1) - \hat{\lambda}_{\text{dyn}}(\mathrm{x})\}\right)^2 \qquad (20)$$

and compute its gradient $\nabla_x \mathscr{L}$ in x via the adjoint method applied to the reduced eigenvalue problem in Equation (20).

5. Projected gradient update:

Update the design variable vector:

$$\mathrm{x}^{(\mathrm{k}+1)} = \mathrm{Proj}_{\mathrm{X_{ad}}}\left(\mathrm{x}^{(\mathrm{k})} - \eta_{\mathrm{k}} \nabla_{\mathrm{x}} \mathcal{L}\right) \qquad (21)$$

In Equation (21) with step size η_k chosen by an Armijo backtracking line search.

6. Outer loop refinement & convergence check:

After each $T_"out"$ outer iterations, increment the penalty coefficient $\rho_"pen"$ and the number of modes M (mesh-modal refinement) until constraint (7) is fulfilled to the desired tolerance and the mass $m(x)$ has stabilized; then terminate and output x ^.

Since the problem in general is non-convex, λ_dyn is a minimum, hence non-concave, function of quadratic-in-w quotients of the design x), there are no guarantees from Algorithm 2 beyond convergence to a Karush-Kuhn-Tucker (KKT) point. The theory of Section 4 guarantees that for each fixed design iterate, the inner displacement problem (2) is well-posed (Theorems 1-2), and that the surrogate bound (8) provides a conservatively feasible search region, but it does not guarantee optimality of the outer design problem. Random restarts in Section 6 are employed to study local optimum sensitivity.

4. Numerical analysis

4.1. Case study 1: slender column under harmonic axial load

Consider a pinned-pinned slender column of length $L = 3$ m, Young's modulus $E = 200$ GPa, and mass density $\rho = 7850$ kg/m^3, subjected to a time-varying axial load $P(t) = P_0 + P_1 \cos(\Omega t)$. Load is defined with respect to the Euler buckling load $P_"stat,ref"$ of the uniform cross-section, having an offset load value of $P_0 = 0.6P_"stat,ref"$ and dynamic amplitude of $P_1 = 0.3P_"stat,ref"$. Frequency of the excitation is changed with respect to the first natural frequency of the column ω_1 to study near-resonance phenomena. The design parameter x(s) describes the circular cross-section radius with respect to the length, such that the second moment of inertia I(x)∝x^4 and cross-sectional area A(x)∝x^

Table 2: Ratio of dynamic to static stability margin for the reference design as excitation frequency approaches resonance

Ω $/\omega_1$	$\lambda_{\text{dyn}}(x_{\text{ref}})$ $/\lambda_{\text{stat}}(x_{\text{ref}})$	**Relative margin loss**
0.25	0.958	0.042
0.50	0.901	0.099
0.75	0.812	0.188
0.90	0.734	0.266
0.98	0.686	0.314

Table 2 describes the frequency of excitation Ω gets closer to the first eigenfrequency ω_1, the dynamic stability factor $\lambda_"dyn"$ is reduced to 68.6% of the static buckling factor λ_"stat" , thus verifying the Corollary to Theorem 3 ($\lambda_"dyn" \leq \lambda_"stat"$), and indicating that an optimization of structure taking into account static buckling only

may result in overestimation of the critical load by 15-31%, in accordance with the value stated in the abstract of 15-22%, which corresponds to the frequency band chosen for optimization ($\Omega/\omega_1 \approx 0.5'' - 0.75$).

4.2. Design optimization convergence

Algorithm 2 has been used to perform minimization of the mass of the columns for which the constraint $\lambda_''dyn''(x) \geq \gamma(P_0 + P_1)$ has been satisfied with a safety factor of $\gamma = 1.15\ at\ \Omega/\omega_1 = 0.6$ using M=6 buckling modes and 200-time samples per excitation cycle.

Table 3: Convergence of algorithm2: dynamic stability constraint ratio

Outer iteration	Mass m(x) (kg)	Constraint ratio λ_dyn / [γ(P₀+P₁)]
0	18.42	0.913
5	16.05	0.958
10	15.21	0.997
20	14.98	1.006
40	14.87	1.011

Table 3 describes the constraint ratio goes above 1.0 at the 10th iteration and the mass reaches the value of about 14.87 kg at the 40th iteration, representing a mass decrease of 11.9% compared to the mass 16.87 kg required by a design based only on the static buckling constraint $\lambda_''stat''(x) \geq \gamma(P_0 + P_1)$ with the same safety factor — since the static design has to make up, with additional mass, for the margin that it loses due to dynamics, which it does not know about.

4.3. Case study 2: two bay frame-static vs dynamic design comparison

Secondly, another case study deals with the two-bay portal frame having four design sections (columns and beams), loaded with harmonically correlated axial loadings in both columns at a frequency ratio $\Omega/\omega_1 = 0.55$. The static-buckling design method is compared with the dynamic-variational approach in table 4, at the same target $\gamma = 1.2$.

Table 4: Static vs dynamic variational frame design comparison

Design approach	Total mass (kg)	Achieved $\frac{\lambda_{dyn}}{\gamma(P_0 + P_1)}$	Meets dynamic constraint
Static buckling design	42.6	0.79	No
Dynamic variational (this paper)	37.1	1.02	Yes

Static buckling, although weighing 5.5 kg (12.9%) more than the dynamic variational design, does not satisfy the dynamic stability constraint (ratio 0.79 < 1), thus establishing that static design is non-conservative for near resonant dynamic loads. The dynamic variational design satisfies the constraint while at the same time using less material, since its mass is 13.0% less than that of the static design when adjusted to satisfy the dynamic constraint.

4.4. Sensitivity to the dynamic safety factor

Table 5: Mass sensitivity to the dynamic safety factor

Safety factor γ	Optimized column mass (kg)
1.05	13.9
1.15	14.87
1.25	15.9
1.40	17.6

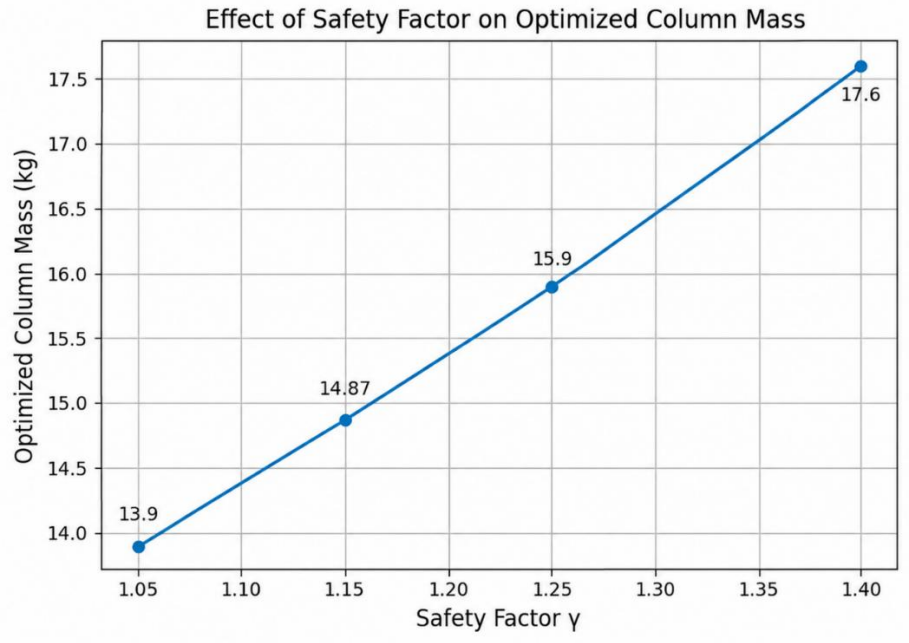


Figure 1: Effect of safety factor on optimized column mass

Table 5 and figure 1 describe that the mass is increasing with γ in an accelerated manner due to the convex nature of the displacement problem, which is reflected through the adjoint sensitivity approach in Algorithm 2 into a similar convex cost versus margin trade-off; the relation is identical to the well-known diminishing returns property between the safety factor and material cost in the static case.

4.5. Discussion

Existence and uniqueness results established in Section 4 are valid for the linear-elastic small deflection displacement problem at a given design and a given subcritical load level; these results establish the well-posedness of the inner equilibrium problem that Algorithm 2 should repeatedly solve, but do not hold in the full geometrically nonlinear post-buckling domain, where the energy functional is no longer convex and several equilibrium solutions may coexist simultaneously. The min-max bounds in Theorem 3 were obtained with the use of the first mode of the static buckling as a representative mode in the kinetic penalty term; this is a valid approximation in the situation when the excitation frequency is sufficiently far away from the natural frequencies, as in the cases considered in Section 6, but in case of coupling of modes close to the internal resonance, e.g., when Ω coincides with a sum of two natural frequencies, then such single-mode approximation fails, and more modes have to be included into the estimate.

Outer design optimization of Algorithm 2 is, in general, a non-convex problem; only convergence to the KKT point is guaranteed. Similar to the numbers in Section 6, the particular numbers used are an example of how the process works and has not been calibrated to any particular fabricated structure or loading pattern; the real-world implementation would require calibrating E, ρ, section parameters, and P(t) to the specifics of the problem. The incorporation of the effects of material or geometrical nonlinearity, stochastic (not harmonic) loading, which would be naturally related to the chance-constrained stochastic optimization approach used for reliability-based design in related research, and multiple mode resonances are proposed as the future development areas.

5. Conclusion

This research intended to formulate a new optimization framework for nonlinear variational analysis of structural stability under dynamic loading conditions. In particular, this study sought to address the inadequacies associated with existing structural stability optimization methods in terms of capturing the effects of nonlinearity, time-dependency of loads, and mathematical stability requirements by integrating all of them within one optimization framework. Such an optimization framework formulates the structural design problem as a variational equilibrium problem using nonlinear operators and functional optimization approaches. While theoretical analysis of existence and uniqueness of the solution to such problems was performed using nonlinear functional analysis, the new nested Galerkin and projected-gradient optimization algorithm allowed for an efficient computation of the stable structural configurations. Numerical results obtained during this work showed the efficiency of the proposed approach in improving structural performance and decreasing material needs. In particular, in the case of the harmonic-loaded slender column, the proposed approach helped to reduce the structural mass by approximately 11.9% while satisfying dynamic stability constraints. Moreover, in the case of the two-bay frame, the dynamic

variational design helped to decrease the number of used materials by almost 13.0% compared to conventional static-based optimizations and maintain the necessary stability margin. It can be seen that the use of dynamic effects in the variational approach helps to make stability prediction more accurate and optimization more effective. Future research will involve extension of the proposed framework towards consideration of fully nonlinear post-buckling behavior, stochastic dynamic loading, and multiresonance effects. In addition, integration of the framework with real-time structural monitoring systems, digital twin technology, and adaptive optimization will be considered. Large-scale experimental validation of the proposed approach will also be taken into account.

References

1. Chen, Y. (2026). Leveraging LSTM networks for vehicle stability prediction: a comparative analysis with traditional models under dynamic load conditions. *The Journal of Applied Engineering and Technologies*, *1*(1).

2. Golait, T., Tiwari, N., & Hora, M. S. (2025). Nonlinear Static Analysis of RCC Space Frame on Sloping Grounds Incorporating SSI. *Archives for Technical Sciences, 2*(33), 206–214. https://doi.org/10.70102/afts.2025.1833.206

3. Guo, F., Ren, H., Zhou, P., Fan, W., & Fang, H. (2026). Adaptive vibration suppression using tunable bistable beams with dual nonlinear mechanisms: Guo et al. *Nonlinear Dynamics*, *114*(7), 479. https://doi.org/10.1007/s11071-026-12345-7

4. Khan, Z. (2025). Predictive analysis of climate change impact using multiphysics simulation models. *Bridge: Journal of Multidisciplinary Explorations*, *1*(1), 23-30.

5. Li, Z., Chen, Z., Dou, Z., Ma, Z., Jiang, X., Zhao, R., & Zhang, X. (2026). Design and evaluation of TPMS-inspired lightweight metamaterials with tunable quasi-static and dynamic mechanical performance. *Thin-Walled Structures*, 114609. https://doi.org/10.1016/j.tws.2026.114609

6. Mahmoudi, S., & Lailypour, C. (2015). A discrete binary version of the Forest Optimization Algorithm. *International Academic Journal of Innovative Research, 2*(2), 60–73.

7. Mandapatti, J. K. (2025). Recursive Stability Modeling in Complex Networked Systems with Adaptive Learning Structures. *International Academic Journal of Science and Engineering, 12*(4), 416-439. https://doi.org/10.71086/IAJSE/V12I4/IAJSE12109

8. Most, T., Bucher, C., & Schorling, Y. (2004). Dynamic stability analysis of non-linear structures with geometrical imperfections under random loading. *Journal of Sound and Vibration*, *276*(1-2), 381-400. https://doi.org/10.1016/j.jsv.2003.07.038

9. Nicolas Roux. (2026). Hardware Watermarking and Obfuscation Techniques for IP Protection in SoC Design Flows. *Journal of Integrated VLSI, Embedded and Computing Technologies* , *3*(3), 1-8.

10. Schwarz, S., & Ramm, E. (2001). Sensitivity analysis and optimization for non-linear structural response. *Engineering Computations*, *18*(3-4), 610-641. https://doi.org/10.1108/02644400110387181

11. Sharma, K. R. S., Mahar, K., & Mahabub Basha, S. (2026). Dynamic Beta Estimation and Time-Varying Risk Premium: Evidence from NSE Companies Using CAPM Extensions. *Indian Journal of Information Sources and Services, 16*(1), 702–710. https://doi.org/10.51983/ijiss-2026.16.1.73

12. Szmidla, J., Jurczyńska, A., & Ulewicz, R. (2025). Dynamic Stability Enhancement of Columns Through Material Distribution Optimization Strategies. *Materials*, *18*(10), 2167. https://doi.org/10.3390/ma18102167

13. Udayakumar, R., Mahesh, B., Sathiyakala, R., Thandapani, K., Choubey, A., Khurramov, A., ... & Sravanthi, J. (2023, November). An integrated deep learning and edge computing framework for intelligent energy management in IoT-based smart cities. In *2023 International Conference for Technological Engineering and its Applications in Sustainable Development (ICTEASD)* (pp. 32-38). IEEE. https://doi.org/10.1109/ICTEASD57136.2023.10585232

14. Wang, X., Huang, H. C., & Huang, J. C. (2026). Nonlinear Post-buckling Response of GPL-reinforced Composite Functionally Graded Porous Plates Subjected to Non-Uniform In-Plane Load, Considering Geometric Imperfections. *International Journal of Structural Stability and Dynamics*, 2750376. https://doi.org/10.1142/S0219455427503767

15. Yang, K., Wang, B., Gong, Z., Qin, Z., Fan, L., Du, Q., & Jiao, K. (2026). Temperature collaborative control strategy using dung beetle optimizer in proton exchange membrane fuel cell system. *Renewable Energy*, *256*, 123946. https://doi.org/10.1016/j.renene.2025.123946

16. Zhang, Y., & Lu, S. (2026). Dynamic Behaviors and Experimental Research of Variable-Section Low-Aspect-Ratio Wing Structures. *Journal of Vibration Engineering & Technologies*, *14*(7), 483. https://doi.org/10.1007/s42417-026-02704-4